Materials Letters xxx (xxxx) 131453

Contents lists available at ScienceDirect

Materials Letters

journal homepage: www.elsevier.com/locate/matlet

Significantly reduced conductivity in strontium titanate-based lead-free ceramics by excess bismuth

Yuanyuan Wang [a, b], Hongbo Liu [b, *], Tingnan Yan [a], Jianwei Zhao [a], Junjie Li [a], Shifeng Guo [c], Shikuan Sun [d], Rong Sun [a], Zhilun Lu [e, *], Dawei Wang [a, *]

[a] Shenzhen Institute of Advanced Electronic Materials, Shenzhen Institute of Advanced Technology, Chinese Academy of Sciences, Shenzhen 518055, China
[b] School of Materials Engineering, Shanghai University of Engineering Science, Shanghai 201620, China
[c] Shenzhen Key Laboratory of Smart Sensing and Intelligent Systems, Shenzhen Institute of Advanced Technology, Chinese Academy of Sciences, Shenzhen 518055, China
[d] School of Material Science and Energy Engineering, Foshan University, Foshan 528000, PR China
[e] School of Engineering and the Built Environment, Edinburgh Napier University, Edinburgh EH10 5DT, UK

ARTICLE INFO

Keywords:
$SrTiO_3$
$BiFeO_3$
Core–shell microstructure
Impedance
Dielectric properties

ABSTRACT

Lead-free dielectric ceramics $0.75SrTiO_3$-$0.25BiFeO_3$ (ST-BF) with an extra amount of bismuth (Bi) are synthesized by the conventional solid-state reaction method. The crystal structures of ST-BF retain pseudo-cubic phase as Bi content increases. The grain size is found to significantly increase from 1.8 to 4.9 μm and then fall to 3.3 μm in the presence of excess Bi, exhibiting a distinct heterogeneous core–shell microstructure. Impedance spectroscopy data indicates that with increasing excess Bi content to 2 mol%, the shell resistivity increases significantly to ~ 9 MΩ cm with the largest volume fraction of the shell/core area, and both the core and shell activation energies are increased, resulting in reduced loss of ~ 0.08 at 1 kHz and high breakdown strength of ~ 140 kV cm^{-1}. This work provides a potential strategy for further improvement of ST-BF for capacitor applications.

1. Introduction

$SrTiO_3$-$BiFeO_3$ (ST-BF) solid solution is of great interest because of its excellent ferroelectric, piezoelectric and multiferroic properties [1–5]. Makarovic et al. showed that (x)BF-(1-x)ST + 1 wt%Mn ($0.7 \geq x \geq 0.57$) exhibited typical ferroelectric loops and high remanent polarization (P_r ~ 30–50 μC cm^{-2}) [6]. Lu et al. recently presented that the 0.01Nb-doped 0.6BF-0.4ST solid solution showed the optimized electro-mechanical properties with a maximum polarization (P_{max}) of ~52.7 μC cm^{-2} and a large electro-strain of ~0.15% at room temperature [7]. However, the majority of studies concentrated on the BF-rich side of ST-BF solid solution, with less emphasis dedicated to the ST-rich side. Researchers have recently explored ST-BF solid solutions with higher ST content, which showed promising potential for capacitor applications. For example, Ren et al. reported that 0.5BF-0.5ST ceramics with 1 mol% Mn substituting Fe showed a P_r of 6 μC cm^{-2} and a remanent magnetization of 0.009 emu/g [8]. Our recent work demonstrated that whereas Nb doping effectively reduced the total conductivity of 0.75ST-0.25BF, the cores remained highly conductive [9]. Excess Bi has been used in previous work to greatly restrict the leakage current or conductivity of $BiFeO_3$-$BaTiO_3$ (BF-BT) [10] and $(Bi_{1/2}Na_{1/2})TiO_3$ (BNT) [11], and has not been employed in ST-BF solid solution.

In this study, the influence of excess Bi on the microstructure, dielectric, ferroelectric and electrical properties of 0.75ST-0.25BF ceramics were studied. Excess Bi could effectively reduce the electrical conductivity, leading to the reduction of dielectric loss (tanδ) and enhancement of breakdown strength (BDS).

2. Experimental

0.75ST-0.25BF-xBi (x = 0.00, 0.01, 0.02 and 0.03) ceramics was fabricated using a conventional solid-state method as reported elsewhere [9]. Bulk density was measured using the Archimedes method. The crystal structure was characterized by X-ray diffraction (XRD, Rigaku Smart Lab). Polished surfaces of the sintered pellets were examined using a scanning electron microscopy (SEM, Apreo 2, Thermo Fisher Scientific) equipped with a backscattered electron (BSE) and en-

* Corresponding authors.
E-mail addresses: bohongliu@gmail.com (H. Liu), Z.Lu@Napier.ac.uk (Z. Lu), wangdawei102@gmail.com (D. Wang).

https://doi.org/10.1016/j.matlet.2021.131453
Received 16 November 2021; Received in revised form 3 December 2021; Accepted 4 December 2021
0167-577/

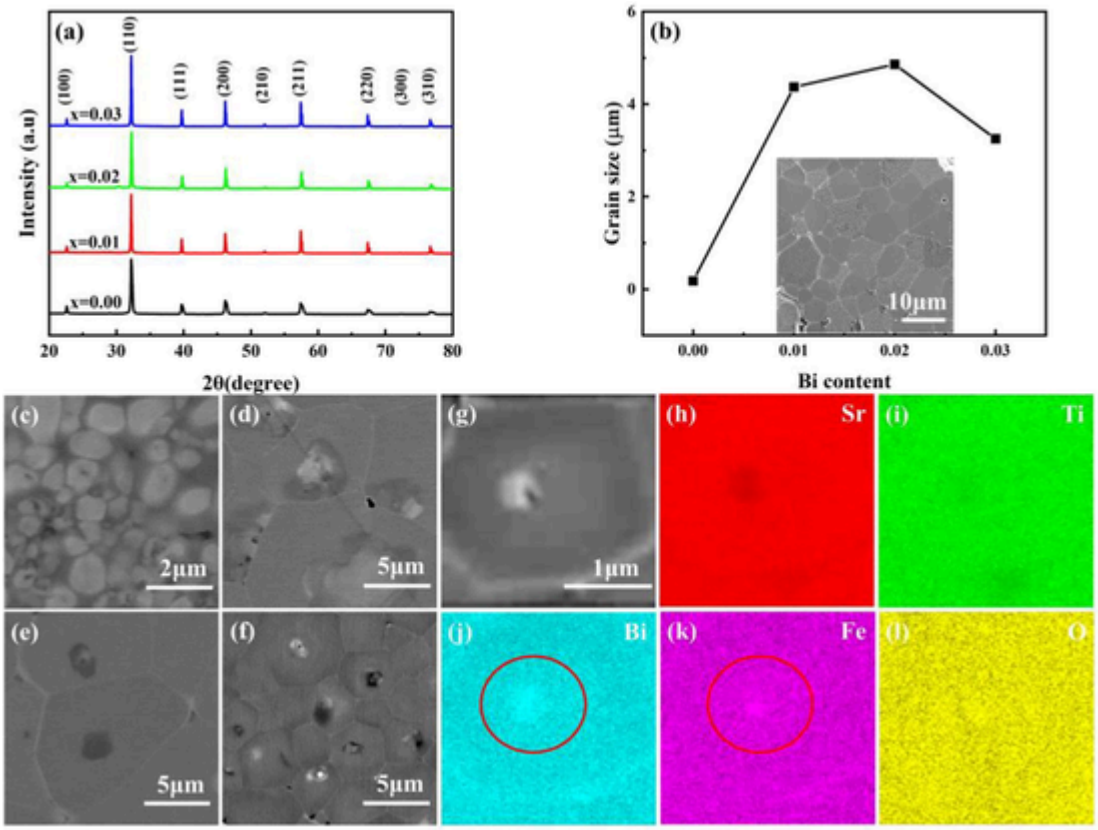

Fig. 1. (a) XRD patterns of ST-BF-xBi ceramics. (b) Average grain size; inset is the SEM image of polished and thermally etched x = 0.02 sample. BSE images of polished surfaces with x = (c) 0.00, (d) 0.01, (e) 0.02, and (f) 0.03. (g) Enlarged image for x = 0.02 with EDS elemental mapping results: (h) Sr, (i) Ti, (j) Bi, (k) Fe, and (l) O.

ergy dispersive X-ray spectroscopy (EDS) detector. Frequency and temperature-dependent dielectric permittivity (ε′) and tanδ were examined using a precision impedance analyzer (Agilent E4980A) from room temperature to 500 °C at 1 kHz, using pellets with coated silver electrodes on opposing parallel surfaces. Polarization-electric field (P-E) loops of pellets were measured via the PK-CPE 1801 High-voltage Test System (PolyK Technologies). Impedance spectroscopy data were rectified using ZView software (Scribner Associates, Inc.) by geometric factors (surface area/thickness, cm).

3. Results and discussion

The crystal structure of ST-BF-xBi ceramic powder is examined by XRD, as shown in Fig. 1a, which reveals a single pseudo-cubic perovskite phase with the $Pm\bar{3}m$ space group without any secondary phase. To refined lattice parameters by Rietveld refinement are listed in Table S1, which exhibited no obvious change. The average grain size is statistically calculated according to the SEM images of different compositions, as displayed in Fig. 1b. With the increase of Bi content, the average grain size is found to significantly increase from 1.8 um to 4.86 um and then decrease when exceeding x = 0.02. Excess Bi addition (x > 0.02) was found to segregate at the grain boundary, hindering the grain growth [9]. BSE images of the polished cross-sections are shown in Fig. 1c-f. A clear core–shell microstructure [12] with a bright and dark contrast is found because of elemental segregation during sintering, with Bi and Fe being abundant in cores and grain boundary (Fig. 1g-l) [13, 14].

Impedance complex plane (Z*) plots for ST-BF-xBi ceramics are shown in Fig. 2a. The total resistivity of ceramics can be obtained from the low frequency intercept on the Z' axis [13]. Non-typical semicircles appear at 50 °C for x = 0.00, which displays that 0.75ST-0.25BF has a large leakage current. However, for x ≥ 0.01 the semicircles can only be observed at high temperature, and the diameter of semicircle increases and reaches a maximum at x = 0.02 and then decreases, revealing that the optimal Bi concentration for the lowest conductivity is 0.02. Combined Z“ and M” spectroscopic plots are shown in Fig. 2b and c, where two peaks can be observed for all samples. Z“ is the imaginary part of Z*. M” was calculated using the equation $M'' = 2\pi f \varepsilon_0 Z'$ (f is the frequency in Hz, $\varepsilon_0 = 8.854 \times 10^{-14}$ F cm^{-1}, and Z' is the real part of Z*). It suggests that there are two electroactive components which can be treated as two parallel resistor–capacitor elements connected in series [15]. These two observed components correspond to the non-typical semicircles in Z* plots (Fig. 2a), revealing excess Bi content does not significantly improve the electrical homogeneity [16]. The values of R and C for each component observed in Fig. 2b, c are listed in Table 1 [9]. It is obvious that adding more Bi significantly increases the resistivity of the shell, reaching a maximum of 8950.80 kΩ cm at x = 0.02. Given that the permittivity of the shell and core remains essentially constant for all ceramics, the volume fraction of the shell/core region reaches a maximum value of 0.45 at x = 0.02 (inversely proportional to the capacitance ratio of shell and core), consistent with the core–shell microstructure shown in Fig. 1.

The Arrhenius plots and activation energies (E_a) of ST-BF-xBi are given in Fig. 2d and Table S2. A small excess of Bi can significantly alter E_a, with E_a of core and shell reaching maximum values of 0.39 eV at x = 0.02 and 1.15 eV at x = 0.03, respectively [17]. The conductivity of the core and shell both decreases significantly as Bi content increasing. The highest shell resistivity combined with the largest shell volume fraction at x = 0.02 may lead to the highest BDS.

The frequency and temperature dependent for ε′ and tanδ of ST-BF-xBi at 1 kHz are presented in Fig. 3a-b. Bi addition improves dielectric properties with the lowest tanδ stable up to 300 °C at x = 0.02. From

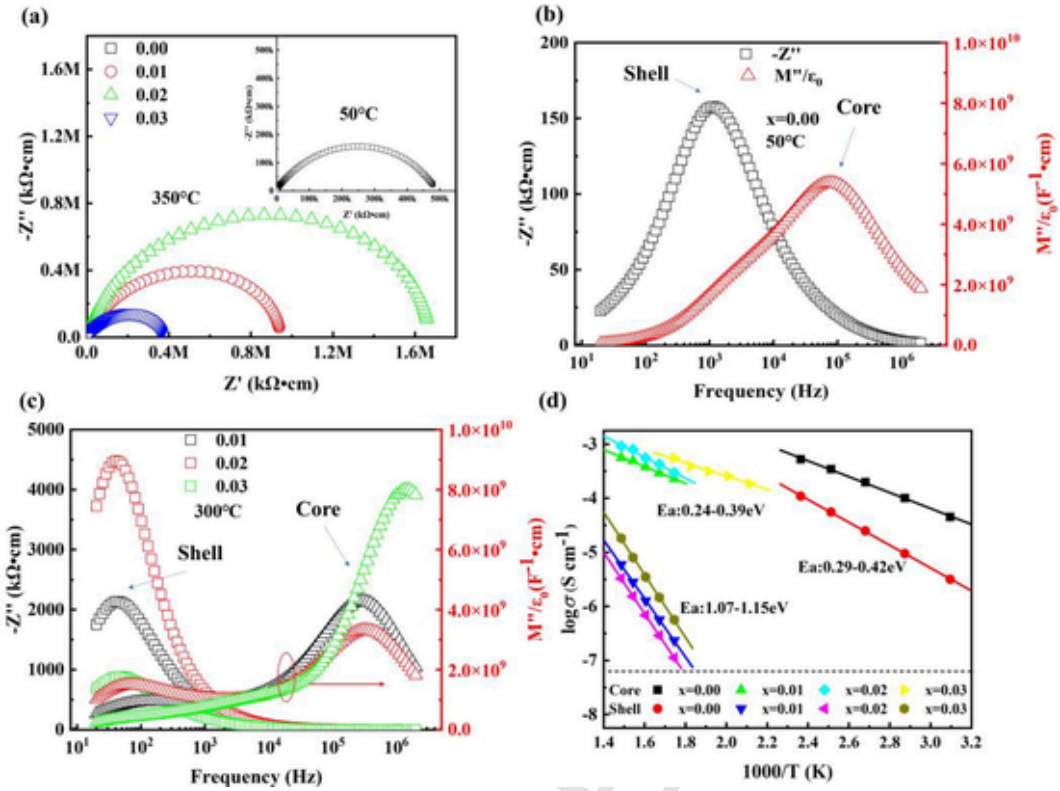

Fig. 2. (a) Temperature-dependent Z* plots for ST-BF-xBi ceramics with x = 0.00 at 50 °C, 0.01–0.03 at 300 °C; Combined Z'' and M'' spectroscopic plots at 50 °C for x = (b) 0.00, at 300 °C for x = (c) 0.01–0.03; (d) Arrhenius plots of ST-BF-xBi ceramics.

Table 1
The values of R and C for each component.

Composition	Component 1 (Shell)		Component (Core)	
	R = 2Z'' (kΩ·cm)	C = 1/(4πfZ'') (F cm^{-1})	R = M''/(ε$_0$πf) (kΩ·cm)	C = ε$_0$/(2 M'') (F cm^{-1})
0.00 (50 °C)	315.36	4.31 × 10^{-10}	22.21	9.30 × 10^{-11}
0.01 (300 °C)	4272	8.26 × 10^{-10}	4.38	1.17 × 10^{-10}
0.02 (300 °C)	8958.80	4.42 × 10^{-10}	3.40	1.5 × 10^{-10}
0.03 (300 °C)	1768.38	1.99 × 10^{-9}	1.80	6.25 × 10^{-11}

being unable to obtain P-E loops for x = 0.00 to being able to endure an electric field of 50 kV cm^{-1} for x ≥ 0.01, the ferroelectric properties have been significantly improved with the decreased leakage current (Fig. 3c). The bipolar P-E loop for x = 0.02 stays slim with increasing electric field up to 140 kV cm^{-1} (Fig. 3d), indicating a high BDS [18, 19].

4. Conclusions

Lead-free ST-BF ceramics with trace additions of Bi elements were prepared, which discovered that excess Bi content had a significant effect on the microstructure and electrical properties. The increase of grain size from 1.8 to 4.86 μm with core–shell structure are related to the addition of Bi compensating for the volatilization. The impedance spectroscopy results indicate that x = 0.02 provides the highest resistivity and the optimal dielectric and ferroelectric properties. The combination of the highest shell resistivity and the largest shell volume fraction results in a maximum BDS of > 140 kV cm^{-1} at x = 0.02.

CRediT authorship contribution statement

Yuanyuan Wang: Conceptualization, Methodology, Writing – original draft. **Hongbo Liu:** Supervision. **Tingnan Yan:** Data curation. **Jianwei Zhao:** Formal analysis. **Junjie Li:** Validation. **Shifeng Guo:** Writing – review & editing. **Shikuan Sun:** Writing – review & editing. **Rong Sun:** Funding acquisition. **Zhilun Lu:** Writing – review & editing. **Dawei Wang:** Writing – review & editing.

Declaration of Competing Interest

The authors declare that they have no known competing financial interests or personal relationships that could have appeared to influence the work reported in this paper.

Acknowledgements

The work is supported by the National Natural Science Foundation of China (11704242), the Construction of Basic Research Institutions from Shenzhen Science, Technology and Innovation Commission and the Natural Science Foundation of Shanghai, China (17ZR1447200).

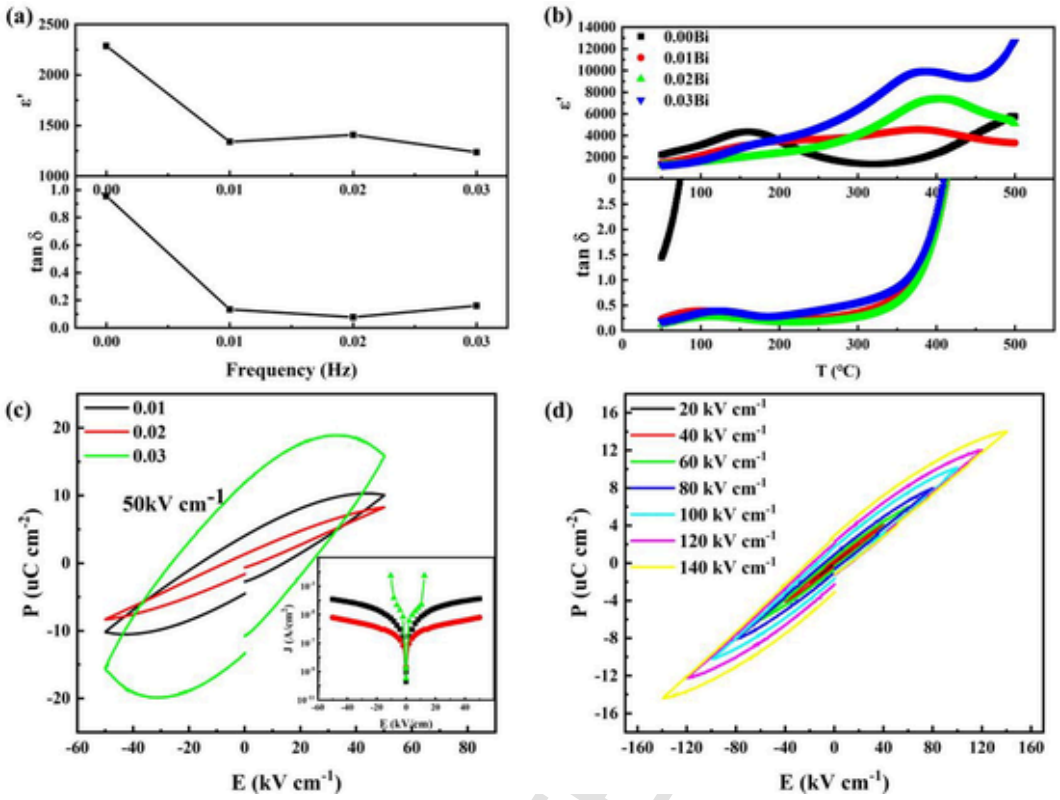

Fig. 3. (a) The frequency and (b) temperature dependent for ε′ and tanδ of ST-BF-xBi at 1 kHz; P-E loops of (c) $0.01 \leq x \leq 0.03$ at 50 kV cm^{-1}, the inset is the corresponding leakage current, and (d) $x = 0.02$ up to 140 kV cm^{-1}.

Appendix A. Supplementary data

Supplementary data to this article can be found online at https://doi.org/10.1016/j.matlet.2021.131453.

References

[1] D.J. Goossens, C.J. Weekes, M. Avdeev, W.D. Hutchison, J. Solid State Chem. 207 (2013) 111–116.
[2] Z.Z. Ma, Z.M. Tian, J.Q. Li, C.H. Wang, S.X. Huo, H.N. Duan, S.L. Yuan, Solid State Sci. 13 (12) (2011) 2196–2200.
[3] S. Vura, P.S. Anil Kumar, A. Senyshyn, R. Ranjan, J. Magn. Magn. Mater. 365 (2014) 76–82.
[4] H. Liu, X. Yang, Ferroelectrics 500 (1) (2016) 310–317.
[5] A. Kumar, A. Kumar, S. Saha, H. Basumatary, R. Ranjan, Appl. Phys. Lett. 114 (2019) 2.
[6] M. Makarovic, A. Bencan, J. Walker, B. Malic, T. Rojac, J. Eur. Ceram. Soc. 39 (13) (2019) 3693–3702.
[7] Z. Lu, G. Wang, L. Li, Y. Huang, A. Feteira, W. Bao, A.K. Kleppe, F. Xu, D. Wang, I.M. Reaney, Mater. Today Phys. 19 (2021) 100426.
[8] Y.P. Ren, H.B. Liu, F.C. Liu, G. Liu, J. Alloys Compd. 877 (2021) 160239.
[9] Y. Wang, H. Liu, T. Yan, J. Zhao, S. Guo, R. Sun, Z. Lu, D. Wang, J. Am. Ceram. Soc. https://doi.org/10.1111/jace.18194.
[10] C. Zhou, H. Yang, Q. Zhou, G. Chen, W. Li, H. Wang, J. Mater. Sci.: Mater. Electron. 24 (5) (2012) 1685–1689.
[11] X.X. Wang, X.G. Tang, K.W. Kwok, H.L.W. Chan, C.L. Choy, Appl. Phys. A 80 (5) (2005) 1071–1075.
[12] B. Zhu, G. Guo, G. Wu, Y. Zhang, A. Dong, J. Hu, D. Yang, J. Alloys Compd. 775 (2019) 776–783.
[13] G. Wang, J. Li, X. Zhang, Z. Fan, F. Yang, A. Feteira, D. Zhou, D.C. Sinclair, T. Ma, X. Tan, D. Wang, I.M. Reaney, Energy Environ. Sci. 12 (2) (2019) 582–588.
[14] D. Wang, Z. Fan, W. Li, D. Zhou, A. Feteira, G. Wang, S. Murakami, S. Sun, Q. Zhao, X. Tan, I.M. Reaney, ACS Appl. Energy Mater. 1 (8) (2018) 4403–4412.
[15] F. Kang, L. Zhang, B. Huang, P. Mao, Z. Wang, Q. Sun, J. Wang, D. Hu, J. Eur. Ceram. Soc. 40 (4) (2020) 1198–1204.
[16] L. Li, T. Roncal-Herrero, J. Harrington, S.J. Milne, A.P. Brown, J.S. Dean, D.C. Sinclair, Acta Mater. 216 (2021) 117136.
[17] Z. Lu, G. Wang, W. Bao, J. Li, L. Li, A. Mostaed, H. Yang, H. Ji, D. Li, A. Feteira, F. Xu, D.C. Sinclair, D. Wang, S.-Y. Liu, I.M. Reaney, Energy Environ. Sci. 13 (9) (2020) 2938–2948.
[18] X. Xie, D. Zhan, Q. Xu, D. Huang, M. Chen, D. Chen, F. Zhang, J. Mater. Sci.: Mater. Electron. 31 (7) (2020) 5305–5315.
[19] H. Ye, F. Yang, Z. Pan, D. Hu, X. Lv, H. Chen, F. Wang, J. Wang, P. Li, J. Chen, J. Liu, J. Zhai, Acta Mater. 203 (2021) 116484.